

## Electronic Spin Transition of Iron in the Earth's Deep Mantle

PAGES 13, 17

Electronic spin is a quantum property of every electron, associated with its intrinsic angular momentum. Though there are no suitable physical analogies to describe the spin quantum number, there are two possibilities, called spin 'up' and spin 'down.' The electronic structure of iron in minerals is generally such that valence electrons will more abundantly occupy different spatial orbitals and maintain the same spin than occupy the same spatial orbital and assume opposite spin, called 'spin-paired.'

To the astonishment of mineral physicists, pressure-induced electronic spin-pairing transitions of iron that were predicted nearly 50 years ago recently have been detected in major mantle-forming oxides and silicates in ultrahigh-pressure experiments at lower-mantle pressures

BY J.-F. LIN, S. D. JACOBSEN, AND R. M. WENTZCOVITCH

[e.g., *Badro et al.*, 2003, 2004; *Lin et al.*, 2005]. If such a spin transition is occurring in the Earth's lower mantle, there may be profound geophysical implications.

This article describes what is known about the nature of the spin transition, focusing on the possible effects on the physical properties of the deep mantle such as seismic velocities and transport properties, as well as on the effects of pressure and temperature on the spin transition interval (Figures 1 and 2). Recent experimental observations and theoretical advances are motivating multidisciplinary efforts to reevaluate the implications of spin transitions on our understanding of the state of Earth's lower mantle.

### Iron in the Mantle

Mineralogical models of the planet indicate that the lower mantle, the most voluminous layer of the Earth, consists of approximately 20% ferropericlase [(Mg,Fe)O] and approximately 80% silicate perovskite [(Mg,

Fe)SiO<sub>3</sub>] containing minor amounts of aluminum, in addition to a small amount of calcium silicate perovskite (CaSiO<sub>3</sub>). Recent studies also show that silicate perovskite may transform to a post-perovskite structure just above the core-mantle boundary (see *Eos* 86(1) pp. 1,5, 2005). Iron (Fe) is the most abundant 3d transition metal in the mantle, substituting for magnesium (Mg) at a level of about 20% in ferropericlase and about 10% in silicate perovskite.

The unique properties of iron give rise to complex physical and chemical properties of Earth's lower mantle. Iron exhibits two main valence states in silicates and oxides: ferrous iron (Fe<sup>2+</sup>) with six 3d electrons and ferric iron (Fe<sup>3+</sup>) with five 3d electrons. The electronic configuration of iron therefore depends on its oxidation state, that is, the number of valence electrons. The spin transition in iron results primarily from the competition between two quantities: the crystal field splitting energy ( $\Delta$ ) and the exchange splitting energy ( $\Lambda$ ).  $\Delta$  is the energy separating the (hybridized) triplet  $t_{2g}$ -like and doublet  $e_g$ -like  $d$ -orbitals in the case of sixfold coordinated iron.  $\Delta$  depends strongly and inversely on the iron-oxygen bond length and thus on pressure, temperature, and composition.  $\Lambda$  is the energy separating  $d$ -orbitals of the same energy with

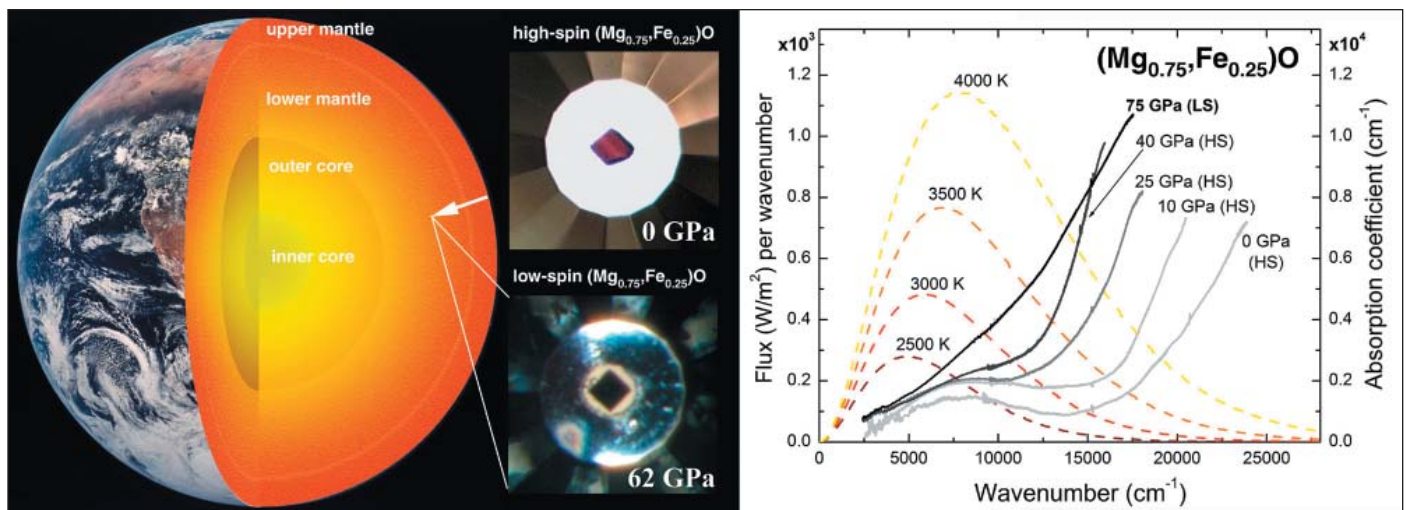


Fig. 1. (left) A cutaway of Earth's interior reveals increasing brilliance of spectral radiance with depth as temperatures increase from approximately 2500 to about 4000 K between the top and base of the lower mantle. (right) Theoretical blackbody emission fluxes at several temperatures are plotted with dashed lines. The absorption of near-infrared and visible light by ferropericlase across the spectral range increases with increasing pressure [after Goncharov et al., 2006]. The change in absorption is readily visible to the naked eye, as seen by viewing single crystals of  $(\text{Mg}_{0.75}\text{Fe}_{0.25})\text{O}$  inside a diamond-anvil pressure cell at ambient pressure in the high-spin (inset top) and approximately 62 gigapascals in the low-spin state (inset bottom).

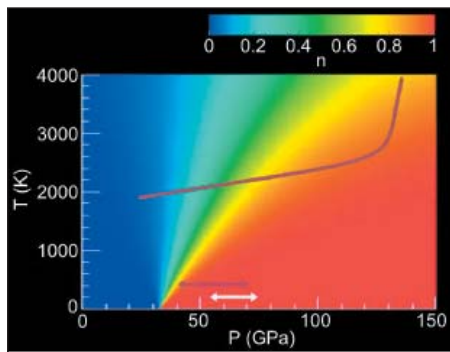


Fig. 2. Spin crossover in ferropericlase  $[(\text{Mg}_{0.8125}\text{Fe}_{0.1875})\text{O}]$  at high pressures and temperatures [Tsuchiya et al., 2006]. The mixed spin states exist in various fractions in the lower mantle. Variable  $n$  is the fraction of the low-spin irons. Experimental transition pressures at 300 K in ferropericlase are denoted by dark brown arrows [Badro et al., 2003] and white arrows [Lin et al., 2005], respectively. The dark brown line is a lower-mantle geotherm.

different spin (spin up or spin down). Under ambient conditions,  $\Delta$  is usually larger than  $\Delta$  and the valence electrons assume a high-spin state (Figure 2).

High-spin  $\text{Fe}^{2+}$  has four unpaired and two paired 3d electrons, i.e., the maximum number of unpaired electrons possible. Under pressure, however,  $\Delta$  increases with respect to  $\Delta$ , and it becomes favorable to occupy orbitals with electrons of opposite spin, that is, to pair electrons. In the low-spin state,  $\text{Fe}^{2+}$  has all six 3d electrons paired (Figure 2). Such a spin-pairing transition in ferropericlase has now been observed experimentally [e.g., Badro et al., 2003; Lin et al., 2005], resulting in new theoretical models of spin states in the Earth's deep mantle [e.g., Sturhahn et al., 2005; Tsuchiya et al., 2006] (Figures 2 and 3).

In practice, the geophysical relevance of this discovery is that low-spin and high-spin iron are like two different chemical species with distinct and unique physical-chemical properties. Under certain circumstances, such as high iron concentration, the spin transition might produce binary loops, that is, the separation of two distinct phases with different bulk compositions. However, it appears that for the low concentrations expected in the mantle the spin transition has a continuous nature (Figure 2), like a second-order transition, involving a mixed population of spins between the high-spin and low-spin end-members.

The low-spin iron phases for ferropericlase and perovskite are not recoverable from high-pressure experiments because the spin transition is reversible. Because of the difference in effective ionic radius between the high-spin and low-spin octahedral  $\text{Fe}^{2+}$ , it also has been suggested that the electronic spin transition in iron in ferropericlase and perovskite would affect the distribution of

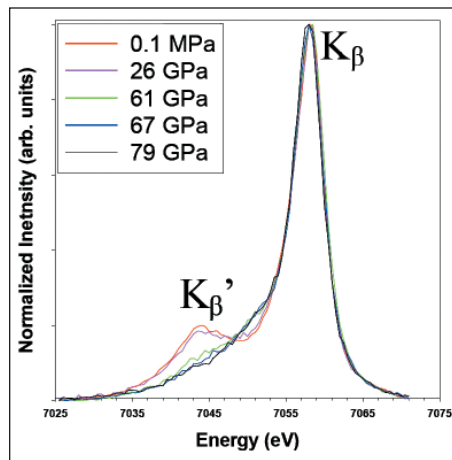


Fig. 3. Experimental observations of the electronic spin-pairing transition of iron in ferropericlase  $[(\text{Mg}_{0.75}\text{Fe}_{0.25})\text{O}]$  under high pressures and room temperature. Representative X-ray emission spectra of  $\text{Fe-K}_{\beta}$  are collected from a single-crystal ferropericlase [Lin et al., 2005]. The presence of the satellite peak ( $\text{K}_{\beta}'$ ) at ambient pressure and 26 gigapascals is characteristic of the high-spin state of iron, whereas the absence of the satellite peak above 61 gigapascals indicates the occurrence of the low-spin ferropericlase.

iron between these two phases [Badro et al., 2003]. However, such conjecture has not been confirmed by experiments in samples with mantle-like composition.

X-ray diffraction and theoretical studies of ferropericlase alone showed a dramatic increase in the incompressibility across the spin-pairing transition [Lin et al., 2005; Tsuchiya et al., 2006], although an accurate model of the pressure-volume relationship requires further study. According to theory [Tsuchiya et al., 2006], the volume of a single iron octahedron is reduced by about 8% across the high-spin to low-spin transition. Sound velocities of ferropericlase rise notably across the spin transition [Lin et al., 2005; 2006], though slowing in sound velocities may be expected within the transition region.

The spin transition in iron is also sensitive to temperature, which should affect the nature of this transition in the mantle, since this region is subjected to high pressures and temperatures (22 gigapascals and ~1800 K at the top of the lower mantle to 140 gigapascals and ~2800 to ~4000 K at the bottom of the lower mantle). Recent theoretical predictions show that the spin transition of  $\text{Fe}^{2+}$  in ferropericlase would occur continuously over an extended pressure range (a spin crossover) under the pressure-temperature conditions of the lower mantle [Sturhahn et al., 2005; Tsuchiya et al., 2006] (Figure 2). Therefore, despite the dramatic changes in compressibility, density, and sound velocities [Lin et al., 2005, 2006; Tsuchiya et al., 2006] in the mantle, this transformation and the associated changes in physical properties should occur quite continuously. This is anticipated to be a

general phenomenon to occur also in perovskite, even though the temperature effect on the spin transition in this mineral is yet to be studied.

Pressure-temperature dependent thermal conductivity is expected to play a role in mitigating large lateral temperature gradients that would otherwise inhibit the stability of seismically observed superplumes [e.g., Hofmeister, 1999; Matyska and Yuen, 2006]. Heat flow in the mantle also should be affected by the spin transition because the radiative component of the thermal conductivity is highly sensitive to the electronic structure. Low-spin ferropericlase exhibits high absorption in the middle- and near-infrared spectral range where a high flux of thermal radiance is expected [Goncharov et al., 2006] (Figure 1).

Spin-pairing transitions in iron-bearing perovskite also have been reported experimentally, though these transitions appear to be more complex than those in ferropericlase. While X-ray emission studies report a two-step, gradual transition of  $\text{Fe}^{2+}$  in perovskite [Badro et al., 2004], results from high-pressure Mössbauer spectroscopy, a technique that is sensitive to the spin and valence states of iron, suggest a continuous transition of  $\text{Fe}^{3+}$  (instead of the dominant  $\text{Fe}^{2+}$ ). Reconciling this inconsistency is crucial for understanding the effects of the spin transitions when modeling lower-mantle properties.

The spin state of iron in the recently discovered post-perovskite phase is another unsettled issue. Many attributes of the electronic transitions in perovskite and post-perovskite are yet to be understood, particularly at the high pressure-temperature conditions of the lower mantle.

### Future Challenges

Considering the spin crossover in ferropericlase and the (possible) two-step spin transitions in perovskite in the lower mantle, it now remains to be seen how results from new measurements at ultrahigh pressures and temperatures will influence geophysical, geochemical, and geodynamic modeling of the lower mantle. More directly related to seismological observation, the effects of the transition on compressional and shear wave velocities through the lower mantle need to be assessed [Lin et al., 2005; 2006]. Though sound velocities are exceptionally difficult to measure experimentally at lower mantle conditions, it is expected that light scattering, ultrasonic, or inelastic X-ray scattering methods soon will make these pertinent data available.

The limited mineral physics data and the lack of consensus on, and understanding of, the nature of this transition in silicate perovskite and post-perovskite are major barriers (as well as golden research opportunities) to modeling satisfactorily the seismic, mineralogical, and geodynamic behavior of the lower mantle. These challenges are stimulating experimentalists and theorists to explore this new frontier collaboratively, generating collateral

benefits to high-pressure mineral physics and the Earth sciences in general. This will generate great collateral benefits to high-pressure mineral physics in general.

#### Acknowledgments

The authors acknowledge C. S. Yoo, V. V. Struzhkin, A. F. Goncharov, W. Sturhahn, J. M. Jackson, D. Yuen, and K. Hirose for stimulating discussions. This work at Lawrence Livermore National Laboratory (LLNL) was performed under the auspices of the U.S. Department of Energy by the University of California/LLNL under contract W-7405-Eng-48. S. D. J. acknowledges support from the U.S. National Science Foundation (NSF; EAR-0440112). R. M. W. also acknowledges support from NSF (EAR-0325218 and ITR-0428774).

#### References

- Badro, J., et al. (2003), Iron partitioning in Earth's mantle: Toward a deep lower mantle discontinuity, *Science*, *300*, 789–791.
- Badro, J., et al. (2004), Electronic transitions in perovskite: Possible nonconvecting layers in the lower mantle, *Science*, *305*, 383–386.
- Goncharov, A. F., V. V. Struzhkin, and S. D. Jacobsen (2006), Reduced radiative conductivity of low-spin (Mg, Fe) O in the lower mantle, *Science*, *312*, 1205–1208.
- Hofmeister, A. M. (1999), Mantle values of thermal conductivity and the geotherm from phonon lifetime, *Science*, *283*, 1699–1706.
- Lin, J. F., et al. (2005), Spin transition of iron in magnesio-wüstite in Earth's lower mantle, *Nature*, *436*, 377–380.
- Lin, J. F., et al. (2006), Sound velocities of ferropericline in Earth's lower mantle, *Geophys. Res. Lett.*, *33*, L22304, doi:10.1029/2006GL028099.
- Matyska, C., and D. A. Yuen (2006), Lower mantle dynamics with the post-perovskite phase change, radiative thermal conductivity, temperature- and

depth-dependent viscosity, *Earth Planet. Sc. Lett.*, *154*, 196–207.

Sturhahn, W., J. M. Jackson, and J. F. Lin (2005), The spin state of iron in Earth's lower mantle minerals, *Geophys. Res. Lett.*, *32*, L12307.

Tsuchiya, T., R. M. Wentzcovitch, C. R. S. da Silva, and S. de Gironcoli (2006), Spin transition in magnesio-wüstite in Earth's lower mantle, *Phys. Rev. Lett.*, *96*, 198501.

#### Author Information

Jung-Fu Lin, Lawrence Livermore National Laboratory, Livermore, Calif.; E-mail: lin24@llnl.gov; Steven D. Jacobsen, Department of Earth and Planetary Sciences, Northwestern University, Evanston, Ill.; and Renata M. Wentzcovitch, Department of Chemical Engineering and Materials Science, University of Minnesota, Minneapolis.

## Looking Below the Moon's Surface With Radar

PAGES 13, 18

Imaging radar observations of the Moon at long wavelengths probe up to tens of meters into the mixed dust and rock of the lunar regolith. These images support geologic studies, mapping of resource-bearing deposits of pyroclastic glasses or titanium-rich basalt, and the search for safe landing sites with ready access to such resources.

A nearly complete map of the lunar nearside at 70-centimeter wavelength has been collected, using the radar transmitter on the U.S. National Science Foundation's (NSF) Arecibo telescope in Puerto Rico and receivers on the NSF's Robert C. Byrd Greenbank Telescope (GBT) in West Virginia (Figure 1). These data have been submitted to the Planetary Data System in a format that makes them useful for a variety of lunar science applications.

The Moon's surface is exposed to bombardment by large and small meteorites, and over time these impacts create a mixed layer of dust and rock fragments called the regolith. Atop the basalt flows (maria) that fill ancient basin floors, the regolith is a few meters thick. In older highlands terrain, the regolith is 10 meters or more in thickness, with significant layering that reflects overlapping ejecta deposits from the major basins and nearby large craters. Remote sensing data in ultraviolet to thermal infrared wavelengths characterize regolith physical properties and composition for the upper few microns to centimeters. Gamma ray and neutron measurements extend the depth of probing to about one meter with, to date, coarse spatial resolution.

Only the drill cores and shallow seismic and electrical surveys made by the Apollo astronauts address the vertical and horizontal variations in the regolith, and for just a few sites on the Moon. Earth-based long-wavelength imaging radar provides a window on near-surface regolith properties across the entire nearside and illustrates the scientific potential of future radar studies of Mars.

#### Lunar Radar Mapping

Earth-based radar maps are produced by measuring echo power as a function of time delay and Doppler shift that can be related to the different distances and velocities, relative to the radar's location, of each point on the lunar surface. The delay-Doppler ambiguity between points north and south of the 'spin equator' is avoided by pointing the Arecibo beam toward just one hemisphere of the Moon. The transmitted radar signals are adjusted to hold a single target point on the Moon at fixed time delay and frequency throughout a 16-minute 'look.' Other sites on the Moon also illuminated by the Arecibo radar signal have different delay and frequency changes with time, and so their reflected energy is 'smeared' over many resolution elements. A 'patch-focusing' technique is used to compensate for these drifts over a region centered on some particular point, and the high-resolution map is assembled from a grid of locally focused images.

The maps have a horizontal spatial resolution along the delay axis of 450 meters per pixel at the limb, and about 900 meters per pixel closer to the center of the disk. Resolution along the frequency axis is 320 meters along the apparent spin axis of the Moon and degrades slowly with increasing angular offsets from the spin vector. The data are

resampled to a lunar cartographic grid at 400-meter spacing.

Arecibo transmits a circularly polarized radar signal, and the GBT is used to receive both reflected senses of circular polarization. These two channels are important because they contain information on mirror-like echoes from locally flat parts of the Moon as well as from diffuse echoes associated with rocks, roughly 10 centimeters and larger, on and within the regolith. The transmitted power and the strength of the GBT thermal noise signal are measured to allow calibration of the echoes to backscatter cross section. The circular polarization ratio (CPR) obtained from the two echo channels is a measure of decimeter-scale rock abundance and can be used to search for thick ice deposits in permanently shadowed regions near the poles. A calibrated data set allows comparison between echoes from lunar geologic features and terrain

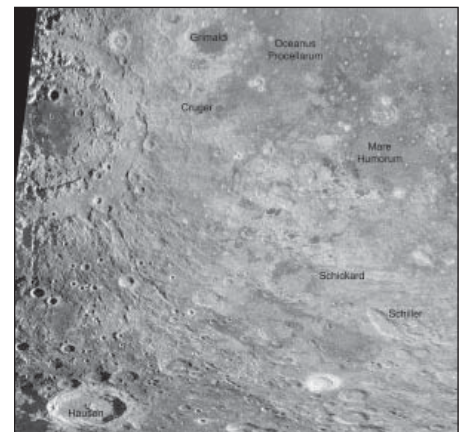


Fig. 1. Seventy-centimeter radar map of the Moon's southwest nearside ( $0^{\circ}$ – $70^{\circ}$ S,  $100^{\circ}$ – $27^{\circ}$ W); same-sense circular polarization. The area of low radar return surrounding Cruger crater and extending northeast to Oceanus Procellarum is likely a deposit of ancient mare basalt buried by Orientale basin debris. The SMART-1 impact site is just south of Mare Humorum.